

Death-associated Protein 3 Localizes to the Mitochondria and Is Involved in the Process of Mitochondrial Fragmentation during Cell Death*

Received for publication, January 5, 2004, and in revised form, May 25, 2004
Published, JBC Papers in Press, June 2, 2004, DOI 10.1074/jbc.M400041200

Zohar Mukamel and Adi Kimchi‡

From the Department of Molecular Genetics, Weizmann Institute of Science, Rehovot 76100, Israel

Death-associated protein 3 (DAP3) was previously isolated in our laboratory as a positive mediator of cell death. It is a 46-kDa protein containing a GTP binding domain that was shown to be essential for the induction of cell death. DAP3 functions downstream of the receptor signaling complex, and its death-promoting effects depend on caspase activity. Recent reports have suggested that DAP3 is localized to the mitochondria, but no functional significance of this localization has been reported so far. Here, we study the sub-cellular localization and cellular function of human DAP3 (hDAP3). We found that hDAP3 is localized to the mitochondria and, in contrast to cytochrome *c*, is not released to the cytoplasm following several cell death signals. Overexpression of hDAP3 induced dramatic changes in the mitochondrial structure involving increased fragmentation of the mitochondria. Both the mitochondrial localization of hDAP3 and its GTP-binding activity were essential for the fragmentation. The punctiform mitochondrial morphology was similar to that observed upon treatment of HeLa cells with staurosporine. In fact, reduction of endogenous hDAP3 protein by RNA interference partially attenuated staurosporine-induced mitochondrial fission. Thus, hDAP3 is a necessary component in the molecular pathway that culminates in fragmented mitochondria, probably reflecting its involvement in the fission process. These results, for the first time, provide a specific functional role for hDAP3 in mitochondrial maintenance.

The mitochondria are a key regulator of mammalian apoptotic cell death. During apoptosis, several apoptosis-inducing factors, such as cytochrome *c*, AIF, Smac/DIABLO, and Endo G are released from the mitochondria and drive several fundamental apoptotic processes, including caspase activation and DNA fragmentation/condensation. The mitochondria also undergo multiple physiologic changes during programmed cell death, including opening of the permeability transition pore, which results in dissipation of the inner mitochondrial membrane potential ($\Delta\Psi_m$), production of reactive oxygen species, and reduction in ATP synthesis (1–4). In addition, recent work has focused on the dramatic alterations in mitochondrial morphology that take place during the early stages of apoptosis

involving fragmentation of the normal tubular network followed by perinuclear clustering of fragmented mitochondria.

Within a cell, mitochondria are in a state of dynamic equilibrium between fusion of individual mitochondria to form a large, single mitochondrion, and fission of mitochondria to smaller organelles. The genes controlling these processes were mostly studied in yeast (for review, see Refs. 5 and 6). Recently it has become apparent that, during apoptosis, there is a disruption in the balance between mitochondrial fission and fusion. Mitochondrial networks are fragmented into small, vesicular, punctiform mitochondria, which may result from the inhibition of fusion, the acceleration of fission, or both (7). Some of the mammalian orthologues of the yeast genes that control the fission/fusion processes have been implicated in apoptosis. These include Drp1 (dynamin-related protein), which regulates outer membrane scission, and Mfn2 (mitofusin 2), a large GTPase that controls fusion of the outer membrane (8, 9). Moreover, it has been recently reported that the pro-apoptotic genes *Bax* and *Bak* affect the mitochondrial ultrastructure and co-localize with Drp1 and Mfn2 to mitochondrial tips and constriction sites where fission events subsequently occur (7, 9).

Here, we analyzed the possible link of another apoptotic gene, death-associated protein 3 (DAP3),¹ to possible changes in mitochondrial morphology. DAP3, a ubiquitously expressed 46-kDa protein, was originally isolated in our laboratory as a positive mediator of interferon- γ -induced cell death in HeLa cells (10). It was also shown to play a more general role in cell death, having an impact on tumor necrosis factor- α and Fas-mediated cell death as well (11). DAP3 contains three potential motifs for GTP binding (12), including the phosphate binding P-loop motif (GXXXXGK(S/T)). In fact, DAP3 binds GTP but not ATP (13). Furthermore, the P-loop is essential for DAP3-induced cell death (11), suggesting that GTP binding is necessary for DAP3 function. DAP3 also contains a putative mitochondrial localization signal within the first 17 amino acids, (14) and, consistent with these structural predictions, the mouse orthologue of DAP3 was found to be localized to the mitochondrial matrix (15). In addition, DAP3 was independently isolated as part of the small subunit of the mitochondrial ribosome in yeast and bovine (*i.e.* mammalian system) (12, 16, 17).

As a cell death-associated protein that has been localized to mitochondria, DAP3 may specifically mediate apoptotic changes of these organelles. In this study, we show that hDAP3 exerts its pro-apoptotic effects from within the mitochondria.

* This work was supported by the Israel Science Foundation and administered by the Israel Academy of Sciences and Humanities and the Feinberg Foundation. The costs of publication of this article were defrayed in part by the payment of page charges. This article must therefore be hereby marked "advertisement" in accordance with 18 U.S.C. Section 1734 solely to indicate this fact.

‡ Incumbent of the Helena Rubinstein Chair of Cancer Research and to whom correspondence should be addressed. Tel.: 972-8-9342428; Fax: 972-8-9316938; E-mail: adi.kimchi@weizmann.ac.il.

¹ The abbreviations used are: DAP3, death-associated protein 3; hDAP3, human DAP3; yDAP3, yeast DAP3; CHO, Chinese embryonic kidney; Δ mito, absence of mitochondrial localization signal; GFT, green fluorescent protein; HEK, human embryonic kidney; Luc, luciferase; mHSP70, mitochondrial heat shock protein 70; MALDI-TOF, matrix-assisted laser desorption/ionization-time of flight; PMS, post-mitochondrial supernatant; STS, staurosporine; siRNA, small interfering RNA.

Furthermore, we found that overexpression of hDAP3 results in mitochondrial fragmentation. Prevention of the mitochondrial localization of hDAP3 or mutation of the P-loop motif that affects the GTP binding activity both abolished the effects of hDAP3 on mitochondrial morphology. This is evidence for a mammalian matrix protein that is involved in the fission/fusion processes, and hDAP3 is among the first few apoptotic proteins to be functionally linked to cell death-associated changes in mitochondrial morphology.

EXPERIMENTAL PROCEDURES

Plasmid Constructions and Transfections—HeLa and HEK 293T cells were transiently transfected by the calcium-phosphate precipitation method, and CHO cells were transfected by LipofectAMINE transfection reagent (Invitrogen). pcDNA3 expressing luciferase (pcDNA3-Luc), hDAP3-FLAG, and hDAP3K134A-FLAG (P-loop mutant) have been described previously (11). A construct of FLAG-tagged hDAP3 that lacks the mitochondrial localization signal (Δ mito) was generated by deletion of the first 51 coding nucleotides. Mito-pDsRed1-N1 (DsRed, a red fluorescent protein targeted to the mitochondrial matrix) and pEGFP expression vectors were obtained from Clontech. The DAP3 siRNA construct was based on the pSUPER vector and was designed as described previously (18); the 19 nucleotide base pairs start at position 474 (the first ATG) of DAP3, and a loop of seven nucleotides was inserted between the sense and antisense sequences.

Immunostaining—HeLa, NIH3T3, and REF52 rodent fibroblasts, A549 human lung carcinoma, primary human foreskin fibroblasts, or CHO cells were grown on 13-mm glass coverslips at a density of $0.8\text{--}1.0 \times 10^5$ cells per 35-mm tissue culture plate. When indicated, $0.1 \mu\text{M}$ of STS (Sigma) or Me_2SO alone was added for 24 h. Cells were fixed in 3.7% formaldehyde for 10 min, permeabilized with cold 100% methanol for 5 min followed by 2 min of 100% acetone drying, and permeabilized/blocked with 0.4% Triton X-100 (Sigma) and 10% normal goat serum (Biological Industries) for 30 min. Mouse monoclonal anti-FLAG antibodies (1:400, M2; Sigma-Aldrich) or mouse monoclonal anti-DAP3 antibodies (1:150; Transduction Laboratories) were applied for 1 h, followed by Cy3-conjugated donkey anti-mouse secondary antibody (1:400; Jackson ImmunoResearch Laboratories) for 1 h. All coverslips were mounted in Fluoromount G (Southern Biotechnology Associates) embedding media. Cells were visualized by either confocal laser-scanning microscopy (Bio-Rad Radiance 2100, mounted on Nikon TE300) or fluorescent microscopy with $60\times$ or $100\times$ oil immersion objectives (Olympus BX41). Digital imaging was performed with a DP50 CCD camera using Viewfinder Lite and Studio Lite software (Olympus). Final composites were prepared in Adobe Photoshop (Adobe Systems).

Analysis of Mitochondrial Morphology—CHO and HeLa cells were transfected for 24 h as described above with 2 or 6.6 μg , respectively, of hDAP3 or control luciferase (Luc) per 35-mm plate. To mark Luc-transfectants, cells were co-transfected with GFP at a 10:1 ratio, whereas hDAP3 transfectants were visualized by further immunostaining with the anti-FLAG antibody as described above. To stain mitochondria, the cells were incubated for 30 min at 37°C with $0.1 \mu\text{M}$ MitoTracker Red CMXRos (Molecular Probes) before fixation. Alternatively, HeLa cells grown on 35-mm plates were transfected with 3.3 μg of Luc, hDAP3, Δ mito, or P-loop and stained with MitoTracker Red and the anti-FLAG antibody 24 h later. In each transfection experiment 100 cells were counted in each of three separate fields, and means \pm S.D. between different fields were calculated. Statistical analysis was performed by two-tailed Student's *t* test.

Cell Fractionation—HEK 293T cells were homogenized in hypotonic buffer (100 mM Tris-HCl, pH 7.4, 250 mM sucrose, and 1 mM K^+ -EDTA) by passing through a 27-gauge needle and centrifuged at $300 \times g$. The resulting supernatant was spun at $12,500 \times g$, generating a post-mitochondrial supernatant (PMS) and a mitochondrial pellet that was resuspended in Ficoll buffer (3% Ficoll, 240 mM mannitol, 30 mM sucrose, 10 mM Tris-HCl, pH 7.4, and 50 mM K^+ -EDTA). This pellet was then passed through a $2\times$ Ficoll buffer column and recentrifuged at $12,500 \times g$. The pellet was suspended in hypotonic buffer and used as a crude mitochondrial fraction. Equal amounts of total protein from each fraction were boiled in loading buffer and resolved by 12% SDS-PAGE.

Co-immunoprecipitation and Proteomic Analysis—For co-immunoprecipitation using extraction buffer (100 mM KCl, 0.5 mM EDTA, 20 mM Hepes, pH 7.9, 0.4% Nonidet P-40, and 20% glycerol), 30 mg of extracts from HEK 293T cells expressing DAP3-FLAG or Δ mitoDAP3-FLAG were incubated for 2 h with FLAG beads at 4°C with gentle agitation. Beads were washed three times with extraction buffer and

twice with high salt buffer (150 mM NaCl, 50 mM Tris, pH 7.9, and 0.5% Triton-X100) and then incubated for 5 min with 100 μl of elution buffer containing FLAG peptide (20 mM Tris, pH 7.3, 150 mM NaCl, and 0.1 mM EGTA). The eluted samples consisting of hDAP3 and associated proteins were subjected to SDS-PAGE, and the gels were stained with GelCode (Pierce). Protein bands of interest were excised from the gel, subjected to trypsin digestion, and analyzed in the Mass Spectrometry Facility of the Weizmann Institute of Science. It consists of a Bruker Reflex IIITM MALDI-TOF mass spectrometer (Bruker; Bremen, Germany) equipped with a delayed extraction ion source, a reflector, and a 337-nm nitrogen laser and API Q-STAR Pulsar¹ electrospray-quadrupole time-of-flight tandem mass spectrometer with a collision cell (MDS Sciex/Applied Biosystems, Toronto, Canada) equipped with a nanoelectrospray source (MDS Proteomics, Odense, Denmark).

Western Blot Analysis—Detection of proteins was performed by standard Western blot analysis using anti-FLAG monoclonal antibodies (M2; Sigma-Aldrich), anti-DAP3 monoclonal antibodies (Transduction Laboratories), anti-mitochondrial HSP70/GRP75 polyclonal antibodies (H-155; Santa Cruz Biotechnology), anti-I κ B- α polyclonal antibodies (C-21; Santa Cruz Biotechnology), or anti-ATP synthase β -subunit polyclonal antibodies (a generous gift from Eiki Kominami, Juntendo University, Tokyo, Japan).

RESULTS

Human DAP3 Protein Is Localized to the Mitochondria—To follow the intracellular localization of the hDAP3 protein, HeLa cells were immunostained with monoclonal antibodies directed to hDAP3. Confocal laser microscopy showed that the endogenous hDAP3 exhibited a punctate pattern of staining (Fig. 1A, left panel) reminiscent of the tubular mitochondrial network. To verify this finding, the cells were co-stained with the specific mitochondrial dye MitoTracker Red CMXRos (Fig. 1A, center panel). Superimposition of the two images revealed a considerable degree of overlap between endogenous hDAP3 staining and the mitochondrial staining (Fig. 1A, right panel). The same pattern of localization was observed in various cell lines of different origins, including human A549 lung carcinoma, human primary fibroblasts, and rodent NIH3T3 and REF52 fibroblasts (Fig. 1B), indicating that the mitochondrial localization is not cell-type specific. The mitochondrial localization was further confirmed by expressing in HeLa cells a mutant of hDAP3 that lacks the putative mitochondrial signal (amino acids 1–17, Δ mito). This mutant showed a diffusible cytosolic staining with no overlap with the MitoTracker staining (Fig. 1C).

The intracellular localization of DAP3 was also studied by biochemical cell fractionation in HEK 293T cells. The cellular extracts were separated into crude mitochondria and PMS fractions. As can be seen in Fig. 1D, the hDAP3 protein was exclusively detected in the mitochondrial fraction, similarly to the mitochondrial protein ATP synthase β -subunit. Neither of these proteins was detected in the PMS fraction, whereas a typical cytosolic protein, I κ B- α , was detected only in the PMS fraction and not in the mitochondrial fraction.

An additional, independent confirmation of the mitochondrial localization of hDAP3 was obtained from an unbiased analysis of hDAP3 interacting partners. Proteins that co-immunoprecipitated from HEK 293T cells with DAP3 or Δ mito (both constructs were FLAG tagged) were resolved by SDS-PAGE, excised from the gel, and identified by mass spectrometry. The pattern of proteins co-immunoprecipitating with wild type hDAP3 was compared with the one obtained by immunoprecipitating the Δ mito, shown to be excluded from the mitochondria. As shown in the left panel of Fig. 1E, although a few bands were common to both forms of hDAP3, one protein of 75 kDa specifically co-immunoprecipitated with the wild type hDAP3 but was absent in complexes of hDAP3, which lack the mitochondrial localization signal (marked by an asterisk). This band was identified upon mass spectrometric analysis as the mitochondrial heat shock pro-

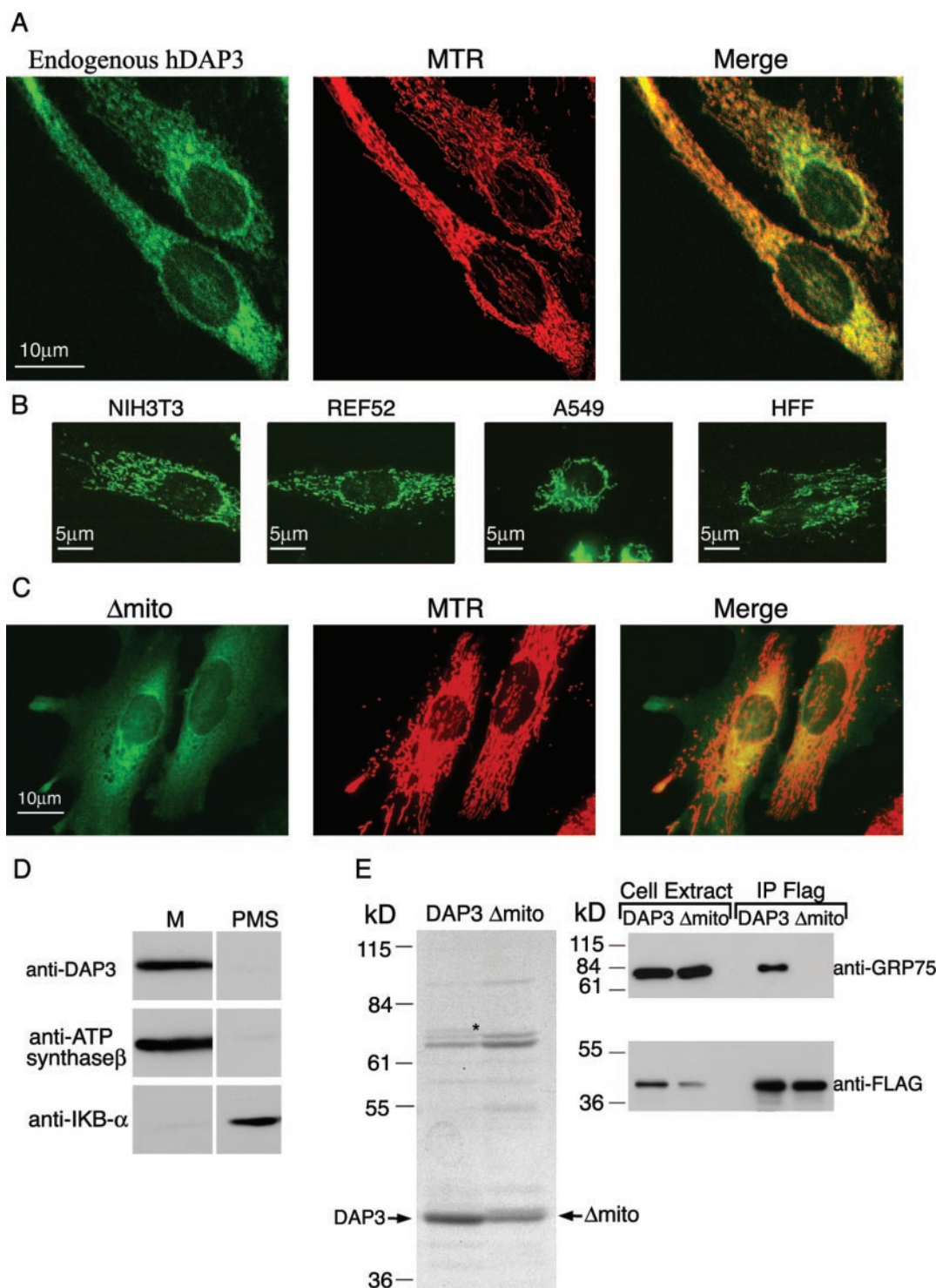


FIG. 1. Localization of hDAP3 to the mitochondria. *A*, confocal imaging of HeLa cells stained with an antibody against hDAP3 (*Endogenous hDAP3*) and with MitoTracker Red CMXRos (*MTR*). Individual images were merged digitally (*Merge*). *B*, localization of endogenous hDAP3 in the indicated cell lines. Cells were stained with an antibody to hDAP3 and viewed by fluorescent microscopy. *C*, HeLa cells were transfected with DAP3FLAG lacking the mitochondrial signal (Δ mito), and were immunostained with anti-FLAG antibodies; this staining was combined with the MitoTracker Red CMXRos (*MTR*), and individual staining was merged digitally (*Merge*). *D*, HeLa cells were fractionated to separate between the mitochondrial fraction (*M*) and the post-mitochondrial fraction (*PMS*). The β -subunit of ATP synthase, I κ B- α , and the DAP3 proteins were detected by Western blotting with the corresponding antibodies. *E*, DAP3 interacts with mitochondrial Hsp70/GRP75. HEK 293T cells transfected with DAP3 or Δ mito were extracted, and lysates were immunoprecipitated with anti-FLAG antibodies (*IP Flag*). The FLAG eluate was loaded onto a 7.5% polyacrylamide SDS gel. The gel was stained with Gel-code reagent to visualize the associated proteins (*left*), and the band denoted with the asterisk was excised from the gels and analyzed by MALDI-TOF mass spectrometry. In parallel, a small portion of these eluted immunoprecipitates (8%) and samples of total cell extracts (50 μ g) were Western-blotted and reacted with anti-FLAG and anti-mHSP70/GRP75 antibodies to detect DAP3 and endogenous mHSP70/GRP75, respectively (*right*).

tein 70 (mHSP70), also named GRP75 (19). Further verification of this interaction was done by Western blotting immunoprecipitates of hDAP3 or Δ mito with an antibody specific to

mHSP70/GRP75 (Fig. 1*E*, *right*). As can be seen, mHSP70/GRP75 was exclusively pulled down by wild type hDAP3 but not by the cytoplasmic form of hDAP3. As mHSP70/GRP75 is

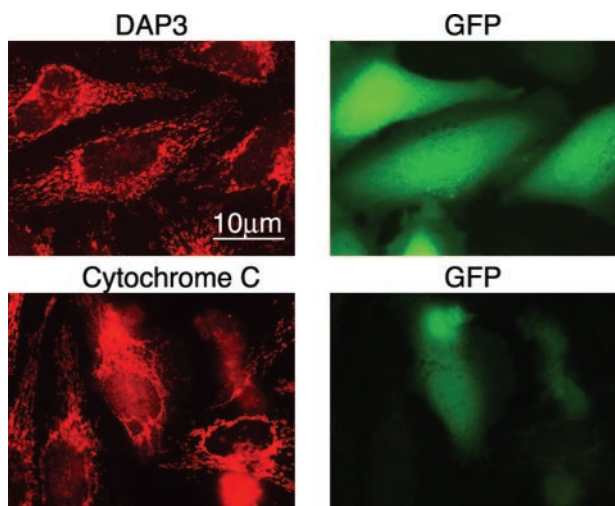


FIG. 2. hDAP3 remains inside the mitochondria during Bax-induced apoptosis. HeLa cells were co-transfected for 24 h with Bax ($0.5 \mu\text{g}$ per 35-mm plate) and GFP in a ratio of 10:1; the green cells in the right panel correspond to the transfected cells. These cells were immunostained with an antibody against hDAP3 or cytochrome *c*, visualized in red (left panel).

directly involved in transporting nuclear encoded protein to the mitochondrial matrix, its interaction with wild type hDAP3, but not cytoplasmic hDAP3, is indicative of the specific import of hDAP3 to the mitochondrial matrix.

hDAP3 Is Not Released from Mitochondria in Response to Bax—Previously identified pro-apoptotic mitochondrial proteins such as cytochrome *c* and AIF exert their apoptotic effects upon release from the mitochondria to the cytoplasm. To determine whether hDAP3 also changes its localization under such circumstances, HeLa cells were transfected with Bax to induce mitochondrial damage and, 24 h later, were stained for hDAP3. Bax-transfected cells were marked by GFP expression (Fig. 2, right panels, green); the fate of hDAP3 in these transfectants was followed by immunostaining with anti-DAP3 antibodies (Fig. 2, top left panel, red). As a positive control, the localization changes of cytochrome *c* were examined in these Bax transfectants using the anti-cytochrome *c* antibody (Fig. 2, bottom left panel, red). The diffuse pattern of cytochrome *c* staining clearly indicated that, as expected, overexpression of Bax leads to the release of cytochrome *c* from the mitochondria. In contrast, however, hDAP3 exhibited the same punctate staining in both transfected and non-transfected cells, suggesting that it remains inside the mitochondria. Similarly, no release of hDAP3 to the cytosol was detected upon treatment of cells with *cis*-platinum (data not shown). The results are consistent with the mouse DAP3 orthologue, previously reported by T. Berger and colleagues (15) to remain inside the mitochondria upon Fas triggering.

Overexpression of hDAP3 Causes Fragmentation of Mitochondria—The fact that hDAP3 remains in the mitochondria during cell death suggests that its pro-apoptotic function takes place within the mitochondria. Because overexpression is sufficient in itself to result in cell death (11, 15), it was interesting to check whether ectopic expression affects any morphological properties of the mitochondria. To this end, hDAP3 or luciferase and GFP were overexpressed in HeLa and CHO cells. hDAP3-transfected cells were stained with anti-FLAG antibody, Luc-transfected cells were marked by GFP (Fig. 3A, green), and the mitochondrial morphology was examined MitoTracker staining (Fig. 3A, red). The normal elongated tubular organization of mitochondria, shown in the luciferase-transfected cells (upper panel), was disrupted in most of the cells that overexpressed hDAP3. Instead, the transfected cells dis-

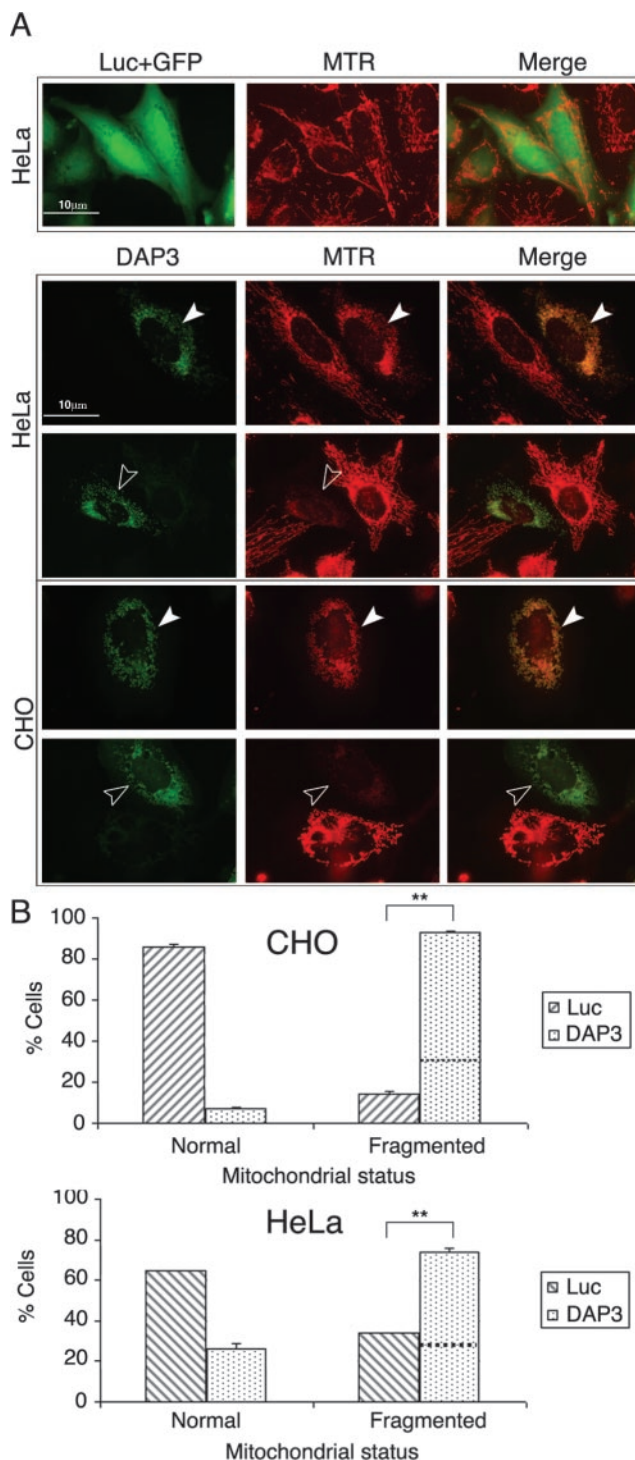


FIG. 3. The involvement of hDAP3 in mitochondrial fragmentation. A, HeLa cells were transfected with hDAP3 or luciferase ($6.6 \mu\text{g}$ per 35-mm plate); CHO cells were transfected with the same plasmids ($2.0 \mu\text{g}$ per 35-mm plate). Both cultures were stained with MitoTracker Red CMXRos (MTR). Transfectants were identified either by staining for FLAG (for hDAP3) or by visualization of co-transfected GFP (for Luc). White arrowheads indicate the DAP3-transfected cells in which mitochondrial fragmentation was detected, and empty arrowheads indicate the cells in which loss of mitochondrial membrane potential was detected as well. B, quantification of the percentage of Luc- or DAP3-transfected cells in which normal or fragmented mitochondrial morphology was detected. Dashed line indicates the percentage of the subpopulation of cells that also exhibit loss of mitochondrial membrane potential. Shown are representative data expressed as the mean \pm S.D. ($n = 3$) from one of three independent experiments with similar results. ** denotes significance level of $p < 0.01$.

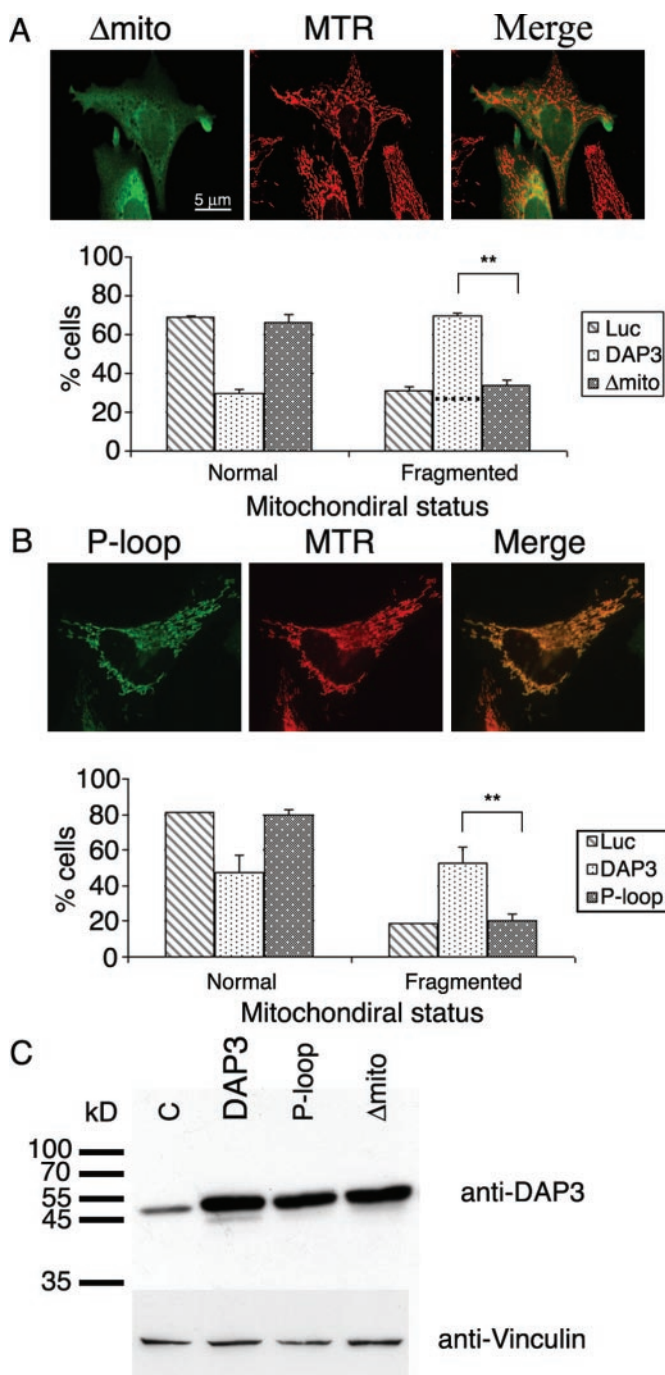


FIG. 4. The effects of hDAP3 on mitochondrial fragmentation require proper mitochondrial localization and the presence of the P-loop motif. A and B, the mitochondrial morphology of HeLa cells transfected with similar concentrations (3.3 μ g per 35-mm plate) of Luc, hDAP3, Δ mito (A), or P-loop mutant (B) was assessed by fluorescent microscopy. The expression pattern of each mutant is shown in the left panels (green), MitoTracker (MTR) staining is shown in the middle panels (red), and the overlap between the two images is shown in the right panels (Merge). Shown are representative data expressed as the mean \pm S.D. ($n = 3$) from one of three independent experiments with similar results. C, expression of each protein was confirmed by Western blot analysis using the anti-DAP3 antibody. The blot was further reacted with an anti-vinculin antibody to normalize for protein loading. ** denotes a significance level of $p < 0.01$.

played punctiform, fragmented mitochondria, which accumulated in the perinuclear area (Fig 3A, white arrowheads). Some of the fragmented mitochondria additionally displayed a loss of membrane potential, as reflected by the reduction in MitoTracker staining (Fig 3A, open arrowheads).

Quantitative evaluation of this phenomenon showed that overexpression of hDAP3 led to mitochondrial fragmentation in 70% and 90% of transfected HeLa and CHO cells, respectively (Fig. 3B). Loss of membrane potential was detected in 30% of the cells that exhibited mitochondrial fragmentation in both cell lines (dashed line within the bar of fragmented mitochondria in Fig. 3B). The effect could be detected as early as 24 h post-transfection, was dose-dependent, and was attenuated by reducing the hDAP3 plasmid concentrations in the transfection process (not shown).

The Correct Intracellular Localization and the GTP Binding Activity of hDAP3 Are Both Essential for the Mitochondrial Fragmentation Induced by hDAP3—To further assess the importance of the mitochondrial localization of hDAP3 for this abnormal mitochondrial morphology, Δ mitoDAP3-FLAG was overexpressed in HeLa cells. Immunostaining of these cells with an anti-FLAG antibody indicated diffuse cytoplasmic staining as shown above, and no changes in mitochondrial morphology were evident. Quantitative assessments showed that the Δ mito did not lead to significant mitochondrial fragmentation over the basal values detected in cells transfected with a control vector (Fig. 4A). In contrast, similar levels of wild type hDAP3 (see Fig. 4C) resulted in mitochondrial fragmentation within 65% of the cells (Fig. 4A). Thus, the mitochondrial localization of hDAP3 is essential for its involvement in mitochondrial fragmentation.

Next, we tested whether the GTP binding activity of hDAP3 is essential for the hDAP3-induced disruption of mitochondrial morphology. To this end, we overexpressed P-loop mutant hDAP3 (Fig. 4B, P-loop) and examined the mitochondrial morphology. The P-loop mutant retained its mitochondrial localization but did not exert any significant effect on mitochondrial morphology (Fig 4B). Western blot analysis confirmed that all of the ectopically expressed proteins (DAP3, Δ mito, and the P-loop mutant) accumulated to the same expression levels (Fig. 4C).

Knockdown of Endogenous hDAP3 Protein Protects against Mitochondrial Fragmentation during Apoptosis—The kinase inhibitor STS, a potent inducer of cell death, triggers mitochondrial fragmentation as a result of increased fission (8). Strikingly, the mitochondrial morphology was similar to the one that is induced by overexpression of hDAP3. To check whether hDAP3 has a critical role during this process, we generated siRNA targeted to hDAP3. An \sim 80% reduction in hDAP3 protein levels was achieved by transfection of HeLa cells for 4 days with pSUPER DAP3 siRNA (Fig. 5A). These cells were then treated for 24 h with STS, and mitochondrial morphology in the transfected cells was assessed by co-transfecting the pSUPER-based vector with the DsRED plasmid. Notably, cells in which hDAP3 protein was reduced were less sensitive to STS, and a greater proportion exhibited normal mitochondria morphology (Fig. 5B).

DISCUSSION

DAP3 is an ancient death-promoting gene whose role in programmed cell death has been conserved from yeast to human. Overexpression of either hDAP3, mouse DAP3, or the *Caenorhabditis elegans* DAP3 orthologue is sufficient to cause cell death (11, 13, 15). In yeast, disruption of yDAP3 prevents induction of cell death triggered by a combination of yeast caspase-1 and hydrogen peroxidase (20). Thus, unlike many apoptotic genes that are not present in the yeast system, DAP3 plays a highly conserved role in programmed cell death.

Despite the extensive work on DAP3, very little information exists concerning the molecular mode of action of this protein. Here, we report for the first time that hDAP3 controls the dynamics of mitochondria morphology and that its overexpres-

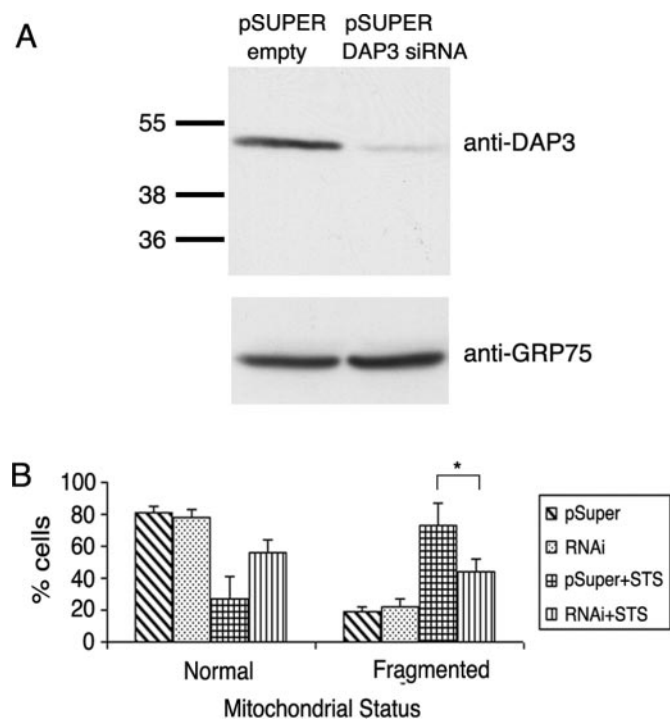


FIG. 5. Reduction of endogenous hDAP3 protein attenuates STS-induced mitochondrial fission. *A*, reduction of hDAP3 protein levels by RNA interference. HeLa cells were transfected with pSUPER or pSUPER containing an siRNA fragment directed against hDAP3 (3.3 μ g per 35-mm plate). After 4 days the cells were lysed, and the hDAP3 expression levels were detected using monoclonal antibodies against DAP3. The mHSP70/GRP75 protein was used as a loading control. *B*, HeLa cells were co-transfected with dsRED (a red fluorescent mitochondrial marker; 0.3 μ g per 35-mm plate) and with either empty pSUPER or pSUPER DAP3 siRNA (3.3 μ g per 35-mm plate). After 4 days, the cultures were treated with STS (0.1 μ M) for 24 h. The mitochondrial morphology was assessed in the transfected cells and scored as the percentage of cells in which normal (elongated) or fragmented mitochondria appeared. Shown for each is the mean \pm S.D. ($n = 3$) from one of three similar independent experiments. * denotes significance level of $p < 0.05$.

sion results in extensive mitochondrial fragmentation, followed by dissipation of mitochondrial membrane potential. This mitochondrial function of hDAP3 is dependent on its intact GTP binding activity, which is consistent with previous reports showing the dependence of the pro-apoptotic effects of hDAP3 on the functionality of this P-loop motif (11, 15). The hDAP3-mediated mitochondrial fragmentation also depends on its correct localization to this organelle, because removal of the N-terminal mitochondrial signal abolished the effects of hDAP3 on mitochondrial morphology. In addition, we show that hDAP3 is retained inside the mitochondria even after transfection with Bax, which causes severe mitochondrial membrane damage, suggesting that hDAP3 acts within the mitochondrion itself. This fits well with the previous localization of DAP3 to the mitochondrial matrix (15) and, more specifically, to the small subunit of mitochondrial ribosomes (12, 16, 17). Our finding that wild type hDAP3, but not its N-terminal truncated form, interacts with mHSP70/GRP75 probably reflects the mechanism through which the nuclear encoded hDAP3 is transported to the mitochondrial matrix. Finally, we show here that STS-induced mitochondrial fission, which is causal to cell death, can be reduced by knocking down endogenous hDAP3 with siRNA, suggesting that hDAP3 is part of the machinery that leads to increased mitochondrial fragmentation during cell death. Because DAP3 siRNA alone does not reduce mitochondrial fragmentation under normal conditions, our data suggest that DAP3 does not regulate mitochondrial fragmentation un-

der homeostatic conditions but rather following cellular stress, upon which it must undergo specific activation. Most likely, this activation state is mimicked by overexpression of DAP3, which is sufficient to lead to fragmentation. Thus, the current study establishes a link between the pro-apoptotic function of DAP3 and its ability to induce mitochondrial fragmentation, providing one of a few existing examples where a death-promoting gene operates in this manner.

Excessive fragmentation of mitochondria can lead to reduction of membrane potential, a phenomenon detected in 30% of the DAP3-mediated fragmented mitochondria. It may also lead to opening of the permeability transition pore and the release of mitochondrial components to the cytoplasm, which is consistent with previous studies that showed cytochrome *c* release in response to murine DAP3 overexpression (15).

Of note, functional studies in yeast further support a mitochondrial function for DAP3. Mutant yDAP3 (Ygl129c) is incapable of growing on glycerol as its sole carbon source, a phenotype typical of disruption of the mitochondria (21). yDAP3 is not directly required for respiration, but in its absence yeast cells tend to lose mitochondrial DNA, suggesting a role in mitochondrial biogenesis (15). It is noteworthy that specific extra-mitochondrial functions have also been attributed to DAP3, including a role in death-inducing signaling complex (DISC) assembly by Trail and Fas receptors via binding to the Fas-associated death domain (FADD), as well as interactions with the glucocorticoid nuclear receptor (13, 22, 23). However, there is still no evidence that endogenous DAP3 localizes to other cellular compartments, which would enable these interactions to occur, and, therefore, the relevance of these observations to the death-promoting effects of DAP3 requires further confirmation.

How can a matrix protein, which is found to be associated with mitochondrial ribosomes, cause mitochondrial fragmentation during cell death? One possibility is that the ribosomal localization reflects a specific function of DAP3 in translational processes within these organelles, which is somehow necessary for the fission/fusion processes. Significantly, high throughput proteomic dissection of ribosomal proteins indicates that DAP3 is the only GTP-binding protein in the ribosome complex (12) and, therefore, could represent the missing GTP binding subunit necessary for translation initiation in the mitochondria. Yet, we were not able to show any functional connection between DAP3 and mitochondrial protein translation (data not shown). The reduction of hDAP3 by siRNA did not alter the overall pattern of protein translation within the mitochondria. Moreover, the effect of hDAP3 on mitochondrial fragmentation was still detected in the presence of chloramphenicol, which specifically inhibits protein translation in mitochondria (data not shown). Other mechanisms that are translation-independent should be investigated in the future. These could include a direct involvement in the fission or fusion processes affecting the mitochondrial inner membrane, which is in the proximity of mitochondrial ribosomes. To date, only one yeast protein, Mdm33, was reported to be involved in the fission of the inner membrane of mitochondria (24), and it will be of interest to test possible interaction between Mdm33 and yDAP3 as well as between the mammalian orthologues. Obviously, a more complete understanding of DAP3 and its function in mitochondria may lead to the elucidation of the fission/fusion process, not only as a cell death phenomenon but also as an essential component of mitochondrial biogenesis and maintenance.

Acknowledgments—We especially thank Dr. Shani Bialik for helpful discussions and reading the manuscript. We also thank Galit Shohat for reading the manuscript. We thank Eiki Kominami for supplying the antibodies against the ATP synthase β subunit.

REFERENCES

1. Martinou, J. C., and Green, D. R. (2001) *Nat. Rev. Mol. Cell Biol.* **2**, 63–67
2. Korsmeyer, S. J., Wei, M. C., Saito, M., Weiler, S., Oh, K. J., and Schlesinger, P. H. (2000) *Cell Death Differ.* **7**, 1166–1173
3. Kroemer, G., and Reed, J. C. (2000) *Nat. Med.* **6**, 513–519
4. Green, D. R., and Reed, J. C. (1998) *Science* **281**, 1309–1312
5. Jensen, R. E., Hobbs, A. E., Cervený, K. L., and Sesaki, H. (2000) *Microsc. Res. Tech.* **51**, 573–583
6. Shaw, J. M., and Nunnari, J. (2002) *Trends Cell Biol.* **12**, 178–184
7. Karbowski, M., and Youle, R. J. (2003) *Cell Death Differ.* **10**, 870–880
8. Frank, S., Gaume, B., Bergmann-Leitner, E. S., Leitner, W. W., Robert, E. G., Catez, F., Smith, C. L., and Youle, R. J. (2001) *Dev. Cell* **1**, 515–525
9. Karbowski, M., Lee, Y. J., Gaume, B., Jeong, S. Y., Frank, S., Nechushtan, A., Santel, A., Fuller, M., Smith, C. L., and Youle, R. J. (2002) *J. Cell Biol.* **159**, 931–938
10. Kissil, J. L., Deiss, L. P., Bayewitch, M., Raveh, T., Khaspekov, G., and Kimchi, A. (1995) *J. Biol. Chem.* **270**, 27932–27936
11. Kissil, J. L., Cohen, O., Raveh, T., and Kimchi, A. (1999) *EMBO J.* **18**, 353–362
12. Cavdar Koc, E., Ranasinghe, A., Burkhart, W., Blackburn, K., Koc, H., Moseley, A., and Spremulli, L. L. (2001) *FEBS Lett.* **492**, 166–170
13. Miyazaki, T., and Reed, J. C. (2001) *Nat. Immunol.* **2**, 493–500
14. Morgan, C. J., Jacques, C., Savagner, F., Tourmen, Y., Mirebeau, D. P., Malthiery, Y., and Reynier, P. (2001) *Biochem. Biophys. Res. Commun.* **280**, 177–181
15. Berger, T., Brigl, M., Herrmann, J. M., Vielhauer, V., Luckow, B., Schlondorff, D., and Kretzler, M. (2000) *J. Cell Sci.* **113**, 3603–3612
16. Suzuki, T., Terasaki, M., Takemoto-Hori, C., Hanada, T., Ueda, T., Wada, A., and Watanabe, K. (2001) *J. Biol. Chem.* **276**, 33181–33195
17. Saveanu, C., Fromont-Racine, M., Harington, A., Ricard, F., Namane, A., and Jacquier, A. (2001) *J. Biol. Chem.* **276**, 15861–15867
18. Brummelkamp, T. R., Bernards, R., and Agami, R. (2002) *Science* **296**, 550–553
19. Schulke, N., Sepuri, N. B., Gordon, D. M., Saxena, S., Dancis, A., and Pain, D. (1999) *J. Biol. Chem.* **274**, 22847–22854
20. Madeo, F., Herker, E., Maldener, C., Wissing, S., Lachelt, S., Herlan, M., Fehr, M., Lauber, K., Sigrist, S. J., Wesselborg, S., and Frohlich, K. U. (2002) *Mol. Cell* **9**, 911–917
21. Tizon, B., Rodriguez-Torres, A. M., and Cerdan, M. E. (1999) *Yeast* **15**, 145–154
22. Hulkko, S. M., Wakui, H., and Zilliacus, J. (2000) *Biochem. J.* **349**, 885–893
23. Hulkko, S. M., and Zilliacus, J. (2002) *Biochem. Biophys. Res. Commun.* **295**, 749–755
24. Messerschmitt, M., Jakobs, S., Vogel, F., Fritz, S., Dimmer, K. S., Neupert, W., and Westermann, B. (2003) *J. Cell Biol.* **160**, 553–564